Biochimica et Biophysica Acta 1828 (2013) 2672–2681

Contents lists available at ScienceDirect

Biochimica et Biophysica Acta

journal homepage: www.elsevier.com/locate/bbamem

Proton-induced endocytosis is dependent on cell membrane fluidity, lipid-phase order and the membrane resting potential

Nadav Ben-Dov [1], Rafi Korenstein *

Department of Physiology and Pharmacology, Faculty of Medicine, Tel-Aviv University, 69978 Tel-Aviv, Israel

ARTICLE INFO

Article history:
Received 28 March 2013
Received in revised form 20 July 2013
Accepted 22 July 2013
Available online 30 July 2013

Keywords:
Endocytosis
Lipid phase order
Membrane surface charge
Membrane fluidity
Resting potential
Actin-cytoskeleton

ABSTRACT

Recently it has been shown that decreasing the extracellular pH of cells stimulates the formation of inward membrane invaginations and vesicles, accompanied by an enhanced uptake of macromolecules. This type of endocytosis was coined as proton-induced uptake (PIU). Though the initial induction of inward membrane curvature was rationalized in terms of proton-based increase of charge asymmetry across the membrane, the dependence of the phenomenon on plasma membrane characteristics is still unknown. The present study shows that depolarization of the membrane resting potential elevates PIU by 25%, while hyperpolarization attenuates it by 25%. Comparison of uptake in suspended and adherent cells implicates that the resting-potential affects PIU through remodeling the actin-cytoskeleton. The pH at the external interface of the cell membrane rather than the pH gradient across it determines the extent of PIU. PIU increases linearly upon temperature increase in the range of 4–36 °C, in correlation with the membrane fluidity. The plasma membrane fluidity and the lipid phase order are modulated by enriching the cell's membrane with cholesterol, tergitol, dimethylsulfoxide, 6-ketocholestanol and phloretin and by cholesterol depletion. These treatments are shown to alter the extent of PIU and are better correlated with membrane fluidity than with the lipid phase order. We suggest that the lipid phase order and fluidity influence PIU by regulating the lipid order gradient across the perimeter of the lipid-condensed microdomains (rafts) and alter the characteristic tension line that separates the higher ordered lipid-domains from the lesser ordered ones.

1. Introduction

Endocytosis usually proceeds via three main steps; inward bending of the plasma membrane, followed by the formation of a connected bud and finally bud scission to form a free vesicle. These steps are commonly governed by curve forming proteins (e.g. BAR and epsin), coat proteins (e.g. caveolin and clathrin) and scission proteins (e.g. dynamin GTPase) [1]. However, endocytic vesicles are also formed when these proteins are inhibited or absent altogether, suggesting that other less defined mechanisms exist. Several clathrin/caveolin independent endocytic pathways have been implicated, such as flotillin coated vesicles, GPI-AP enriched compartments (GEEC) and others pathways which are characterized by their dependence on small G proteins, i.e. RhoA, CDC42 or ARF6 [2,3].

The possible involvement of the physico-chemical properties of the phospholipid polar heads, such as their charge, has been suggested to affect membrane curvature in model lipid bilayers [4,5]. The curvature of the lipid bilayer membrane is primarily expressed through the spontaneous curvature of each monolayer in the coupled bilayer. The decrease in the surface charge density of only one layer is expected to enforce the membrane to adopt a new curvature [6,7]. The electrostatic repulsion between membrane phospholipid polar-heads modulates the area each polar-head occupies, while not affecting the packing order of the lipid hydrocarbon tails [8]. Hence, the local tension produced by a surface area asymmetry between the two membrane monolayers, can be rebalanced by the bilayer adapting its spontaneous curvature, since the equilibrium curvature of a membrane is the product of minimizing the membrane elasto-static and electro-static energies [4,5,9,10]. It has been theoretically argued that for a critical value of membrane surface charged density, the membrane will spontaneously bud in the absence of any applied external force [11,12].

Recently we have shown, using fluorescent and electron microscopies, flow cytometry and spectrometry, that receptor-independent endocytic-like events can be triggered by exposing the cells to external pH < 6 which leads to a highly enhanced proton-induced-uptake (PIU) of macromolecules, in the absence of specific receptor ligands or fusion peptide [13,14]. Fluorescent optical sections clearly demonstrated the homogeneous distribution of the dextran cargo in the cytosol due to an efficient endosomal escape, while the fast recycling of membrane vesicles was supported by TEM experiments [13]. Moreover, we have validated flow cytometry as the quantitative method for the uptake of the dextran by employing enzymatic and quenching methods for

* Corresponding author. Tel.: +972 3 6406042; fax: +972 3 6408982.
E-mail addresses: nadavbe4@tx.technion.ac.il (N. Ben-Dov), korens@post.tau.ac.il (R. Korenstein).
[1] Present address: Dept. of Biotechnology and Food Engineering, Technion Institute of Technology, Haifa, Israel.

0005-2736/$ – see front matter © 2013 Elsevier B.V. All rights reserved.
http://dx.doi.org/10.1016/j.bbamem.2013.07.027

removing residual adsorbed dextran from the cell content analyses. The insensitivity of PIU to inhibiting agents of the known endocytic pathways and to ATP depletion, suggests that PIU proceeds via a new route [13]. Lowering the cell's pH induced partial disruption of the actin cytoskeleton in adherent cells and PIU was shown to depend on cytoskeleton reorganization [15]. Limited disruption of actin membrane scaffolds allows for enhanced PIU, but severe depolymerization of actin filaments impedes it [15]. The suggested mechanism for the initiation of PIU was attributed to the ability of the high proton concentrations at the external surface of the plasma membrane to neutralize part of the negative charge of the phospholipid polar-heads, thus reducing their electrostatic repulsion and consequently the area occupied per molecule. The surface asymmetry that develops across the plasma membrane in terms of surface area and charge density creates an electro-mechanic disparity, reflected by enhanced membrane tension [16], can be balanced by the membrane adapting a new conformation to its spontaneous curvature. This effect was demonstrated in studies where a pH jump triggered spontaneous vesicle formation from planar dispersions of phospholipid acid (PtdOH) [17] and the exposure of composite phospholipid vesicles to localized pulses of low pH was shown to produce the formation of inward tubular membrane invaginations [18–20]. We theorize that the membrane tension will thermodynamically favor the development of membrane invaginations in places where negative curvature values pre-exist, such as in tension lines at the border membrane microdamains of high lipid packing order [8].

In the current study we show that membrane lipid parameters such as phase order and fluidity affect the extent of PIU. We suggest that this effect is mediated by the tension energy associated with the borderline of ordered lipid microdomains.

2. Materials and methods

2.1. Solutions and reagents

Modified Karnovsky's fixative solution (2× strength), 6% paraformaldehyde, 1% glutaraldehyde and 0.2% Triton X-100 in 0.2 M cacodylate buffer; MES buffered saline (MBS), 0.1 mg/ml CaCl, 0.1 mg/ml MgCl–$6H_2O$, KCl 0.4 mg/ml, NaCl 8 mg/ml, 2.06 mg/ml MES (2-(N-morpholino)ethanesulfonic acid, hemisodium salt) and 2 mg/ml Glucose–H_2O, titrated with HCl to pH 5.2.

70 kD Dextran-FITC, Phalloidin-TRITC, Tergitol-40 (nonylphenol ethoxylate), DMSO (dimethylsulfoxide), 6KC (6-keto 3-hydroxy cholesten), MβC (methyl-β-cyclodextrin), Phloretin, Laurdan (6-dodecanoyl-2 dimethylaminonaphthalene), Cholesterol-MβC (40 mg per 1 g MβC) and TMA-DPH (1-(4-Trimethylammoniophenyl)-6-diphenyl-1,3,5-hexatriene) were purchased from Sigma-Aldrich, Rehovot, Israel.

BCECF-AM (2′,7′-bis-(2-carboxyethyl)-5-(and-6)-carboxyfluorescein-acetoxymethyl ester) were purchased from Invitrogen, CA, USA).

2.2. Tissue culture

PBS (phosphate buffered saline), PBS (Ca^{+2} and Mg^{+2} free), DMEM (Dulbecco's Modified Eagle Medium, 4.5 mg/ml glucose), RPMI 1640 (Roswell Park Memorial Institute) culture media, HBSS (Henk's balanced salt solution), FCS (fetal calf serum), trypsin solution (0.25% with 0.05% EDTA), PSN (penicillin 10,000 unit/ml, streptomycin 10 mg/ml, nistatin 1250 unit/ml) L-glutamine solution (200 mM), HEPES (4-(2-hydroxyethyl)-1-piperazineethanesulfonic acid, 1 M) and Tryphan-blue (0.4%), were purchased from Biological Industries, Beit Ha'emek, Israel). Human keratenocytes (HaCaT [21]) were cultured in DMEM, supplemented with 2 mM L-glutamine, 10% FCS and 0.2% PSN solution and were grown at 37° C, in a humid atmosphere of 5% CO_2 in air. Cells were harvested before reaching ~80% confluence by employing trypsin solution for 5 min at RT. The harvested cells were centrifuged for 2 min at 400 *g*. The supernatant was aspirated and the cell pellet was re-suspended in fresh growth media.

Whenever required, iso-osmolarity (290 mOs) of buffer solutions verified by osmometer (Wescor Vapro 5520, Logan, UT, USA).

2.3. Determination of Intracellular pH

The pH-dependent spectral shifts exhibited by BCECF allow calibration of the pH response in terms of the ratio of fluorescence intensity at 535 nm when using two different excitation wavelengths $\lambda_1 =$ 490 nm and $\lambda_2 =$ 440 nm [22]. BCECF-AM is a non-fluorescent, cell permeable derivative that is transformed by intracellular esterase into the charged, non-permeable and fluorescent BCECF molecule.

Calibration curve for BCECF excitation ratio, presented in Table 1a, shows the relative shift in the ratio of BCECF fluorescence in solution as a function of measured pH (Mettler-Toledo SevenEasy pH electrode, Columbus, OH, USA). Cell loading with 10 μM BCECF-AM was performed by incubating the cells for 30 min in HBSS at 37 °C. Following the incubation period, the cells were centrifuged at 400 *g* for 1 min, the solution aspirated, and the cells re-suspended in PBS. For analysis of intracellular pH, the cells were transferred to black 96 well microplates and their emission ratio at 535 nm was determined when excited at 430 nm and 490 nm, respectively (Molecular Devices M5^e, Sunnyvale, CA, USA). Table 1b shows that within 3 min from introducing 20 mM acetic acid into the wells (lowering of the external solution pH to 5), the cells possessed a stable cytoplasmic pH of 5.

2.4. Uptake studies

For the studies of adherent cultures, cells were seeded on surface treated 24 well plates and incubated in growth medium at 37 °C humid atmosphere with 5% CO_2. Experiments were performed when cells reached approximate confluence (~5×10^5 cell/well). In studies of cells in suspensions, harvesting the cells was performed before they were subjected to the treatment protocol. Cell cultures in wells were washed twice with PBS before being subjected to the experimental procedure. During the experiments, each well or vial contained 250 μl of the designated test solution. Termination of the acidic exposure was accomplished by adding 1 ml of cold DMEM into each well or vial, thus recovering the physiological pH of 7.4. Experiments were planned and conducted in a manner that enables all wells in a single plate to enter the washing step at the same time. The wells were washed twice with cold PBS and the cells were harvested by 10 min incubation with a mixture of 0.25 ml trypsin solution and 0.25 ml PBS (deprived of Ca^{2+} and Mg^{2+}) at room temperature. The harvested cells from each well were transferred to a 5 ml vial containing 1 ml cold DMEM with 10% FCS. The cells were washed twice by centrifugation and the cell pellets were re-suspended in 0.5 ml cold PBS. The fraction of cells with compromised membrane integrity was determined during FACS analysis by their disability to exclude trypan-blue from their cytoplasm (5% ± 3%, n = 300 samples).

For uptake studies involving cells enriched or depleted of cholesterol, the cells were incubated in the presence of 0.1 mM cholesterol or 10 mM MβC, respectively, for 45 min at 37 °C, followed by centrifugation (2 min at 400 *g*) and re-suspension in 0.3 ml of either PBS or the MBS. For uptake studies with amphipathic molecules, the cells were

Table 1a
Calibration of BCECF ratio to pH.

pH of BCEF sol.	BCECF Fl ratio	Shift in Fl ratio
7.4	7.352 ± 0.173	
6.5	3.997 ± 0.021	0.544
6	2.830 ± 0.022	0.385
5.4	2.343 ± 0.008	0.319
5.05	2.208 ± 0.01	0.300

Table 1b
Intracellular pH of cells incubated in pH 5 acetic buffer.

Incubation	BCECF-AM FI ratio	Intracellular pH
0 min	1.673 ± 0.012	
3 min	0.511 ± 0.006	5.06
4 min	0.515 ± 0.007	5.03
8 min	0.512 ± 0.003	5.05

divided into separate vials, centrifuged and re-suspended in 0.3 ml of either PBS or MBS. 1% DMSO, 0.7% Tergitol, 90 μM Phloretin or 90 μM 6KC were added to the designated vials for additional 10 min incubation. The cells, suspended in the separate vials, were incubated in the presence of 10 μM dextran-FITC (70 kD) for 10 min, which was terminated by the addition of 1 ml cold PBS and moved to ice. The cells were washed twice by centrifugation with the cells pellets being re-suspended in 0.5 ml cold PBS.

2.5. Flow cytometry (FACS)

Flow cytometry measurements were carried out with FACScalibur (Becton@Dickson, San Jose, CA, USA), employing a 488 nm argon laser excitation. FITC fluorescence was detected by 530/30 nm filter (FL1) and the fluorescence of trypan-blue (TB) was detected by a 680/30 nm filter (FL3). 10,000 cells were collected from each sample and analysis of data was performed in terms of geometrical mean using cyflogic 1.2.1 (CyFlo LTD, Finland) application software. In preparing for FACS analysis, the cells were washed twice in PBS by centrifugation at 400 *g* for 1 min (Du-Pont Sorvall RT6000D, FL, USA). Shortly before FACS analysis, we added to each cells' test tube 0.01% (TB), which served both for quenching the fluorescence of extracellular FITC [23] and for staining necrotic cells with compromised membranes. Cells labeled by TB were rejected from analysis. Microscopic examination of the cells verified the absence of any detectable fluorescent corona associated with the cell membrane. To eliminate signals due to cellular fragments, only those events with forward and side scatter comparable to untreated cells were analyzed.

2.6. Fluorescence measurements

Trimethyl ammonium derivative of diphenyl hexatriene (TMA-DPH), anchor the fluorescent label to the membrane's water–lipid interface, and restrict its diffusion into intracellular membrane organelles. TMA-DPH fluorescent anisotropy (r) (λ_{Ex} 360 nm, λ_{Em} 430 nm), which is inversely proportional to membrane fluidity, was determined using the expression $r = (I_V - GI_H)/(I_V + G2I_H)$ where I represents the fluorescence intensity, V and H represent the vertical and horizontal orientation of the emission polarizers, and G accounts for the sensitivity of the instrument. In order to eliminate the contribution of scattered light by the cells to the measured anisotropy, a density of 2×10^5 HaCaT cell per 200 μl well was chosen, corresponding to $O.D._{340nm} = 0.3$, and a correction factor was determined from samples of unstained cells, as described by Kuhry [24].

Laurdan fluorescent emission is shifted with proportion to the membrane phase properties through its sensitivity to the interaction with the dipolar water molecules. Laurdan fluorescence (λ_{Ex} 350 nm) is represented by its generalized polarization (GP), calculated using the expression $GP = (I_{440} - I_{500})/(I_{440} + I_{500})$, where I is the emission intensity of the laurdan at λ_{Em} 440 nm and λ_{Em} 500 nm which corresponds to its emission maxima in lipid ordered and lipid disordered phases, respectively [25].

All light measurements were carried in a plate reader (Molecular Devices M5^e, Sunnyvale, CA, USA) with automatic determination of G values. 10^6 HaCaT cells were suspended in 1 ml aliquot (PBS or MBS) to which 5 μM TMA-DPH or 5 μM Laurdan were added from a 5 mM stock solutions (in DMSO or methanol, respectively). Each aliquot was divided into four independent 200 μl wells in a black 96 wellplate. The maximal cellular fluorescence intensity was reached 10 min after the addition of the fluorescent probe. The wellplate was placed in the plate-reader with internal temperature set to 25 °C. Prior to each spectral measurement, the well's temperature was determined directly using a thin-wire thermocouple (CHY 508BR, Taiwan). The experiment was stopped after 30 min to minimize the possible fluorescent signal contributed by staining of intracellular membranes [24].

Assessment of the cell membrane integrity was performed by adding 10 μg/ml PI per well and analyzing the cells' fluorescence (λ_{Ex} 480 nm; λ_{Em} 590 nm).

For temperature-dependent measurements, the cells were suspended in cold buffer solution (PBS or MBS) before the addition of TMA-DPH, transferred to pre-cooled black 96 wellplate and kept on ice until placed in the plate-reader (preset to 37 °C). The wells' temperature and polarized fluorescence were recorded every 4 min.

For cells' analysis in the presence of amphipathic molecules, the cells were suspended in PBS and incubated at 37 °C for 45 min in the presence of either 10 mM MβC or 0.1 mM cholesterol (as saturated MβC formulation) or, alternatively, for 10 min with either 1% DMSO, 0.7% Tergitol, 90 μM phloretin or 90 μM 6KC. TMA-DPH and laurdan are virtually colorless in the aquatic phase, however, the presence of residual amphipathic molecules in the solution will lead to a high non-specific background. To overcome this situation, the cells were washed in cold PBS, before the addition of the fluorescent probes. Under this procedure the cells retain stable fluorescence polarization for 30 min at 25 °C while their solution has no contribution to the background fluorescence.

2.7. Fluorescence microscopy

For acquiring images of surface adherent cells, cultures were grown on glass cover slips coated with 2% gelatin. Following fixation with modified karnovsky solution and post-stain with phalloidine-TRITC, cell cultures were optically analyzed. Digital images were acquired by fluorescent microscope (Axio-observer Z1, Zeiss, Germany) equipped with high definition gray scale camera and processed by axiovision software (Zeiss, Germany). Annotation was made using Illustrator CS software (Abode, USA).

3. Results

3.1. The effect of membrane resting potential on PIU

The acidification of the extracellular medium leads to an altered chemical potential gradient of protons across the plasma membrane (ΔpH). The increased hydrogen-ion chemical gradient can produce a depolarization effect on the transmembrane electric potential ($\Delta\psi_m$) through pH induced K^+ membrane conductance [26–28]. Therefore, our first goal was to examine the impact of changes in $\Delta\psi_m$ and ΔpH on PIU.

The dependence of PIU on the resting potential ($\Delta\psi_m$) of the HaCaT cells was explored by replacing the extracellular NaCl with either KCl, choline-chloride (ChCl) or sucrose, while maintaining the iso-osmolarity of the medium. By varying the extracellular concentrations of Na^+ or K^+ ions, one alters the electrochemical potential in the extracellular compartment leading to change in the resting potential, $\Delta\psi_m$. Uptake experiments performed with cultures were incubated for 10 min in the different ion modified HBSS solutions (Table 2), before their pH was brought down to 5.2 using MES acid titration. For conducting the experiment in suspension, the cells were harvested shortly before the experiment and likewise incubated in modified HBSS. Next, the cells were further exposed to the modified solutions for 15 min, in the presence of 10 μM dextran-FITC (70 kD) and the extent of uptake was measured by flow cytometry (Fig. 1). The results demonstrate that membrane depolarization increased the extent of PIU in adherent cell cultures, by up to 100%, depending on the level of

Table 2
The shift in cell membrane potential as function of extracellular ion composition.

Extracellular ions [mM] (modified HBSS) [a]	Na^+	K^+	Cl^-	Choline	Sucrose	Direction of $\Delta\psi_m$ shift [b]
HBSS-MES	140	5	150	–	–	At rest
KCl modified	75	70	150	–	–	Depolarized
KCl modified	15	130	150	–	–	Depolarized
Choline modified	70	5	150	70	–	Hyperpolarized
Sucrose modified	70	5	80	–	140	Hyperpolarized

[a] Ions concentrations are approximated from solution formulations.
[b] Direction of membrane potential was estimated based on Goldman–Hodgkin–Katz (GHK) equation.

Na^+/K^+ substitution, whereas membrane hyperpolarization decreased PIU by 25%, all compared to PIU by cells with unperturbed resting potential. However, when the experiment was repeated with suspended cells (pH 5.25 for 15 min, in the presence of 10 μM, 70 kD dextran-FITC), the level of PIU was found to be unaffected either by depolarization or by the hyperpolarization of the resting potential ($P > 0.05$). The uptake of dextran at pH 7.4 during the short duration of exposure (10 min) is tenfold lower than that taking place at pH 5.2. Thus, due to poor signal/noise ratio, the modulation of uptake by altered resting potential at neutral pH was too low to be determined. The transformation of an adherent cell into a suspended one is accompanied by a major structural reorganization of the cytoskeleton, involving the disruption of stress fibers. Our previous findings [15] that the actin cytoskeleton is an important element in controlling PIU, raises the possibility that in the adherent cells, the change in the transmembrane resting potential initiates remodeling of cytoskeletal structures. To validate this possibility, HaCaT cells, grown on glass cover slips, were incubated in depolarizing or hyperploarizing solutions (70 mM KCl and 70 mM choline modified media, respectively) and stained with phalloidin-TRITC. The fluorescence images of the cytoskeletal actin structures demonstrate a dependence of filamentous actin organization on membrane potential. Cells incubated in HBSS (pH 7.4) are dominated by numerous thick actin stress fibers that transverse across the cell (Fig. 2A). However, cells incubated in a solution that promotes membrane depolarization lack those thick actin fibers (Fig. 2B). In addition, cell–cell contact areas are dominated by fine actin fibrils, perpendicular to the plane of the plasma membrane (Fig. 2B, small arrows) and the cortical mesh at the cell–solution interface is retarded (Fig. 2B, large arrows). Cells incubated in a solution which promotes membrane hyperpolarization (Fig. 2C) have likewise impaired actin stress fibers but are dominated by actin fiberils tangential to the membrane plane (Fig. 2C, large arrows).

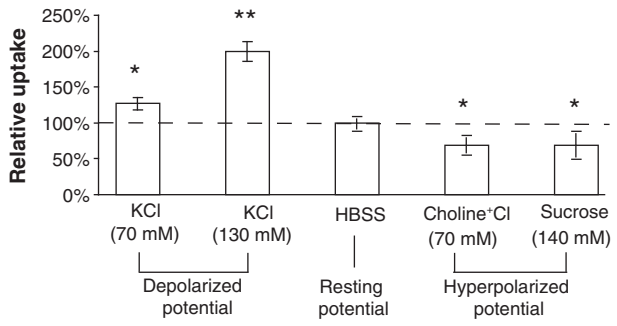

Fig. 1. PIU as function of extracellular cations composition. The medium of HaCaT cultures was replaced by modified HBSS, in which NaCl was replaced by other molecules, i.e. KCl, Choline-Cl or sucrose, while preserving iso-osmolarity (Table 2). Intracellular dextran-FITC intensity is given relative to results obtained from cells exposed to pH 5.25 in standard HBSS salt composition, represented by the horizontal broken line. The cultures were exposed to pH 5.25 or pH 7.4 in the presence of dextran-FITC and were analyzed by FACS, where the geometric mean of fluorescence intensity was determined for each exposure condition. *$P < 0.05$ and **$P < 0.01$, by two-tail *t*-test, $n = 9$ for each treatment, acquired in 3 independent experiments.

3.2. The dependence of PIU on transmembrane proton concentration gradient

The role of the proton gradient (ΔpH) across the membrane on PIU was carefully studied, as we initially expected it to have a substantial effect. We have previously reported that when the cells are exposed to pH 5.25 using MES buffer solution, their cytoplasmic pH drops to 6.5 [13]. In addition, we have shown that acidification of the cytoplasm triggers partial severing of the actin cytoskeleton, which affects the rate of PIU by adherent cells but not by suspended ones [15]. Therefore, experiments concerning the dependence of PIU on ΔpH were conducted with cells in a suspended state. Abolishing the pH gradient across the cell membrane was accomplished by lowering the extracellular pH using an acetate buffer instead of our standard use of the MES buffer. Acetic acid, being a weak acid has the potency to clamp the pH across the cell's membrane [29].

ΔpH was determined by measuring the intracellular pH at a given extracellular one. The assessment of intracellular pH was performed using the pH fluorescent probe of BCECF [22], as detailed in the methods (Tables 1a, 1b). For studying PIU as function of ΔpH, suspended HaCaT cells were exposed to acetate buffer solution (pH 5.25) for 10 min in the presence of 10 μM dextran-FITC (43 kD). For comparison, cells were exposed to the presence of identical dextran-FITC in pH 5.25 MBS buffer or in PBS (pH 7.4). Following the exposure treatment the cells were collected, washed and their cellular fluorescence analyzed by FACS (Fig. 3). The results show that cells acquired comparable dextran-FITC fluorescence intensity when exposed to the lower pH, independent of the transmembrane pH gradient.

3.3. The dependence of PIU on temperature

The dependence of PIU on temperature was studied in the range of 4–36 °C. For reliable measurement of the influx rate, devoid of errors introduced by the temperature dependent efflux, all cells were first treated with 10 μM verapamil, a potent non-specific inhibitor of efflux pumps [30]. The uptake experiments were performed by incubating the cells for 10 min in the presence of dextran-FITC (10 μM, 43 kD) in MBS or PBS solutions, thermally equilibrated in advance at each of the following temperatures: 4, 9, 12, 16, 20, 24, 28 or 36 °C. The contribution of constitutive uptake of dextran-FITC at pH 7.4 was subtracted from all results. To normalize all independent experiments to the same scale, the cells' geometrical mean fluorescence intensity is presented relative to that of cells of the 36 °C group (representing relative uptake of 100%). The dependence of uptake on temperature (Fig. 4A) reveals a linear relationship between the uptake and temperature ($R^2 = 0.99$) in the range of 4–36 °C. The apparent activation energy associated with the uptake process was estimated by the Arrhenius equation via plotting the natural logarithm of the internalization rate (uptake/cell) versus the inverse of temperature (1/°K) yielding an apparent activation energy of 9.25 Kcal/mol.

The averaged anisotropy of phospholipids in the cell's plasma membrane as function of temperature was studied both at a physiological pH (pH 7.4) and at acidic one (pH 5.2). HaCaT cells were harvested, washed, suspended in PBS (pH 7.4) or MBS (pH 5.2), cooled to 5 °C and incubated with 5 μM TMA-DPH. The cells were transferred to black 96 wellplate and their fluorescence polarization and temperature were recorded every 4 min for a 20 min period. At the end of the experiment, no damage to the cells' membrane integrity was found, based on the PI membrane permeability assay. The mean anisotropy of the cells' membrane phospholipids as function of temperature and pH is detailed in Fig. 4B. The data shows that membrane anisotropy has a linear correlation with cells' temperature in the range of 5 °C to 32 °C ($R^2 = 0.87$). The variation in external pH (7.4 to 5.2), in the tested temperature range, does not produce significant difference in the anisotropy of the cell membrane. The fluorescence anisotropy of DPH, which reflects the rate of its molecular rotational motion, represents the inverse of fluidity.

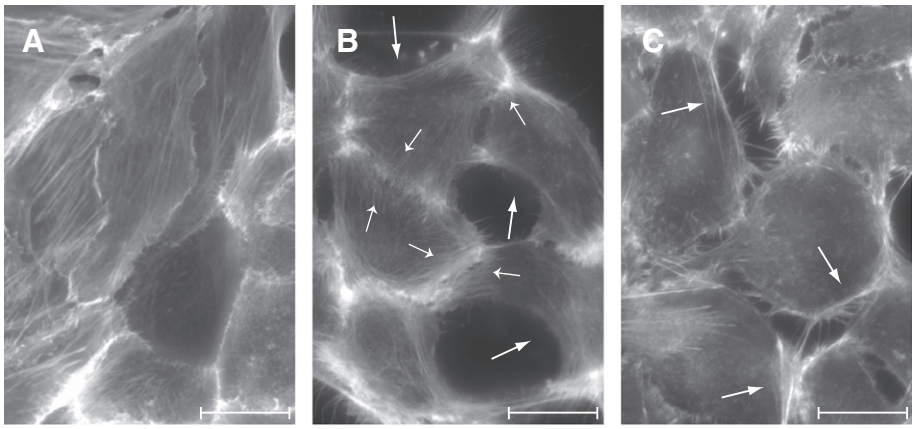

Fig. 2. Actin cytoskeleton remodeling in response to changes in the cell's resting potential. Cell cultures, grown on glass cover-slips, were treated at standard pH 7.4 by (A) PBS, (B) 70 mM choline PBS or (C) 70 mM potassium PBS. The cells were fixed by modified Karnovsky fixative solution and post-stained with phalloidin-TRITC. Cell images were acquired by fluorescent microscopy employing Ex: 540 nm/Em: 580 nm long pass filter at x100 magnification, N.A. = 1.25 (Scale bar = 20 μM). Arrows point to (B, small arrows) fine actin fibrils perpendicular to the plan of plasma membrane, (B, large arrows) retarded cortical mesh at the cell–solution interface and (C, large arrows) condensed actin fibers, tangential to the membrane plane.

Fluidity, described as the freedom of fluid for movements [31], refers in phospholipid bilayer membranes, to the orientation and dynamic properties of the lipid hydrocarbon chains in the bilayer [32].

3.4. The effects of cell membrane's fluidity and phase parameters on PIU

For studying the relationship between membrane fluidity, lipid phase order and PIU, we have chosen to employ chemical agents that can modify these characteristics of the plasma membrane. Experiments were conducted with suspended cells to minimize the possible modulation of the uptake efficacy by the cytoskeleton [15], enabling the lipids' state in the plasma membrane to be the major variable.

In order to detect possible changes in the ratio between ordered and disordered lipid domains in the plasma membrane following the extracellular acidification, we employed the fluorescent probe Laurdan due to its sensitivity to the lipid packing order. The maximum emission wavelength of Laurdan shifts from about 440 nm to about 500 nm upon change of its local lipid environment from an ordered lipid domain into a disordered one. This spectral shift reflects the differences in the number and mobility of water molecules present at the level of the phospholipids glycerol backbones [25]. In the moderate pH 5.2 used in our experiments, the plasma membrane shows no significant alteration of Laurdan general polarization (GP) when compared to cells exposed to pH 7.4 (3% ± 6% at 25 °C, n = 12). These results are in agreement with previous reports [16,19,25].

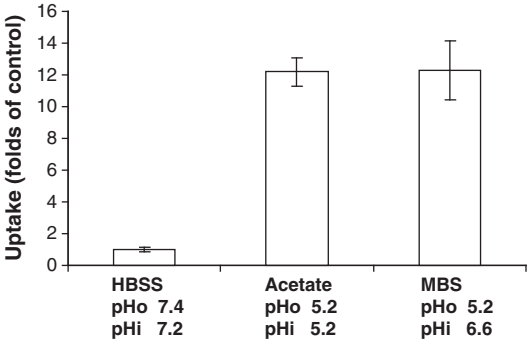

Fig. 3. PIU is not retarded by acidification of the cytoplasm. Suspended HaCaT cells were exposed to acetate buffer (pH 5.2), MES buffer (pH 5.2) or PBS (pH 7.4) solutions for 10 min in the presence of dextran-FITC. Intracellular dextran-FITC intensity is presented relative to control cells exposed to pH 7.4 in HBSS. Results were obtained by FACS analyses and the geometrical mean fluorescence intensity of all cells was determined for each exposure condition. $^{**}P < 0.01$ by two-tail *t*-test, n = 10, acquired in 2 independent experiments.

To examine the dependence of PIU on membrane order parameters, we employed several chemical modifiers of the cell's membrane lipid phase, consisting of cholesterol (entrapped in MβC, 0.1 mM), MβC (10 mM), Tergitol (0.7%), DMSO (1%), phloretin (90 μM) and 6KC (90 μM). Low concentrations of the surfactants Tergitol and DMSO, as well as those of phloretin, 6KC, MβC and cholesterol-MβC were found to have no effect on the plasma membrane permeability as determined by the inability of the hydrophilic PI to penetrate into the cells. At an external concentration of 1 mM cholesterol-MβC, the cell's membrane becomes compromised, as evident from PI permeation, probably due to the severe decrease in membrane fluidity. The cells were exposed to

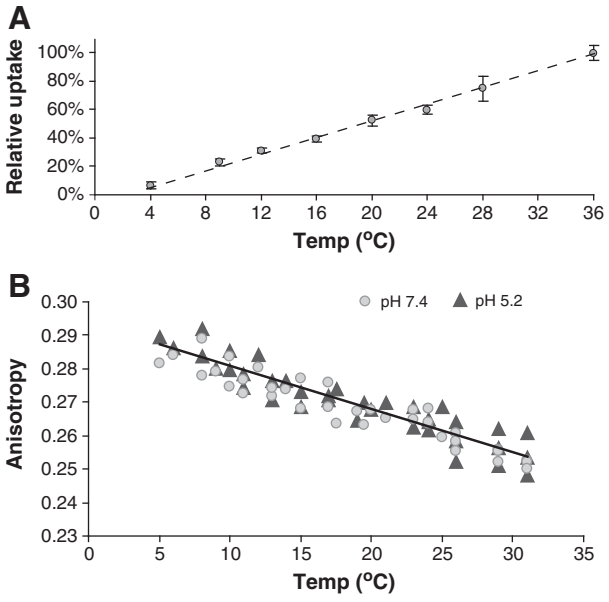

Fig. 4. PIU and membrane fluidity as a function of temperature. (A) Uptake experiments were performed by incubating the cells for 10 min in solution of either pH 5.25 or pH 7.4, in the presence of dextran-FITC. Dextran-FITC uptake was analyzed by FACS and the geometrical mean intensity of all cells is presented relative to that of cells in the 36 °C group (representing 100% uptake). $R^2 = 0.99$. n = 12 for each temperature, acquired in 4 independent experiments. The experimental values are given as mean ± SD. (B) Cell membrane fluidity was determined by measuring steady-state fluorescence anisotropy of cells labeled with TMA-DPH in the temperature range of 5–32 °C. The fluorescence anisotropy of the cells is comparable for pH 7.4 (PBS solutions, circles) and pH 5.2 (MBS solutions, triangles) over the whole temperature range, based on a paired *t*-test ($P < 0.05$, n = 25 acquired in 4 independent experiments) and is linearly correlated with temperature ($R^2 = 0.87$).

the presence of these amphipathic agents for 10 min prior to the onset of PIU, to ensure that possible amphipathic-driven uptake has ceased [33] and allowing the time for the molecules to redistribute into the plasma membrane. Studies based on a number of different techniques indicate that lipid–lipid interactions are generally weak and massive phase separations are not to be expected in phospholipid membranes without the stabilizing contribution of proteins [34].

The relative changes in the cell's membrane fluidity (fluorescence anisotropy of TMA-DPH), lipid packing (GP of laurdan) and uptake (dextran-FITC intensity) are given as the percent of deviation in amphipath-treated cells relative to the values retrieved from control cells i.e. (treatment − control)/control. The membrane fluidity and its GP provide us with important insight into the changes undergone by the plasma membrane. The deviation in anisotropy is presented in Fig. 5A for enriched cholesterol (+9.1%), depleted cholesterol (+6.2%) and for the presence of Tergitol (+7.9%), DMSO (+9.2%), phloretin (insignificant 1.5%) and 6KC (−2.5%). The deviations in lipid packing order are presented in terms of GP values in Fig. 5B for cell's membrane enriched with cholesterol (+33%), depleted of cholesterol (−26%) and for cell's membrane in the presence of Tergitol (−35%), DMSO (−17%), phloretin (no significant change) and 6KC (−7%).

Estimation of the ability of the plasma membrane to undergo inward invagination and vesiculation in response to the cells' exposure to low pH was accomplished through quantifying the extent of PIU, as previously shown [13]. The effect of the different amphipaths on PIU was studied by exposing the cells in MBS (pH 5.2) for 10 min in the presence of dextran-FITC and the specific amphipath. Control cells were exposed under the same conditions in the absence of amphipaths. The change in the geometrical mean of cell fluorescence, reflecting the uptake of dextran-FITC, relative to control cells, is presented in Fig. 5C for cells

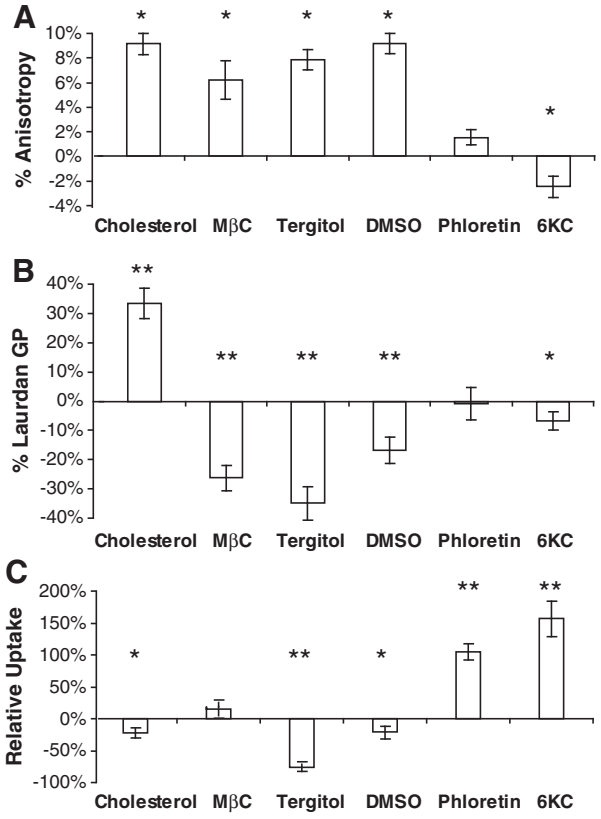

Fig. 5. Changes in membrane fluidity, lipid order and PIU in the presence of amphipathic agents. Results are presented as percent deviation of the data between treated cells and untreated control cells, employing: (A) TMA-DPH fluorescence anisotropy (membrane fluidity); (B) General Polarization of Laurdan (membrane lipid order). (C) Uptake of dextran-FITC analyzed employing FACS. * $P < 0.05$, ** $P < 0.01$ two-tail *t*-test, n = 12 per treatment agent, acquired in 4 independent experiments.

enriched with cholesterol (−22%), depleted of cholesterol (insignificant) and for cells in the presence of Tergitol (−77%), DMSO (−20%), phloretin (+105%) and 6KC (+156%).

4. Discussion

4.1. PIU is indirectly affected by the membrane resting potential

The findings presented in Fig. 1. reveal that membrane depolarization increases the extent of PIU in adherent cell cultures, whereas membrane hyperpolarization decreases PIU compared to the unperturbed resting potential of the cells. However, when the experiment was repeated with cells in a suspended state, PIU was found to be independent of changes in the resting potential. This is in line with a recent finding showing that changes in cytoskeleton architecture affect the efficacy of PIU [15]. Based on the images presented in Fig. 2, we suggest that depolarizing membrane potential weakens and hyperpolarizing strengthens the actin sub-membrane strata and through it influences the membrane bending resistance. The lack of PIU variation in suspended HaCaT cells upon change of the membrane resting potential is attributed to the absence of structural cytoskeleton characteristics typical of adherent cells. This proposal is supported by previous reports demonstrating a similar cytoskeleton remodeling as a function of the plasma membrane potential in diverse epithelia [35–37]. The molecular paths that connect cytoskeleton sensitivity to membrane potential were suggested to include voltage-sensitive membrane proteins and/or peripheral proteins sensitive to surface potentials [38]. The correlation between the observed remodeling of the actin network and the extent of PIU further supports our previous findings [15] that the loss of actin stress fibers increases PIU, whereas the compaction of actin cortex towards the plasma membrane is likely to decrease the deformability of the plasma membrane leading to the attenuation of PIU. In this study we examined whether a shift in membrane resting potential will change the extent of PIU. Our results imply that the membrane potential does not directly intervene in PIU (as is evident from its lack of effect on suspended cells) but can have an indirect effect through its influence on the cytoskeleton organization.

The substitution of the extracellular Na^+ by a non-charged solute such as sucrose, leads not only to membrane depolarization but also alters its surface potential. The reduction of the ionic strength in the vicinity of the external leaflet of the plasma membrane, upon replacing Na^+ by sucrose, causes the widening of the Gouy-Chapman layer of counterions in contact with the cell's glycocalix [39]. However, when comparing PIU of cells treated with sucrose modified solution with that of choline modified one (Fig. 1) no significant change can be found. This is in line with a previous study showing that enzymatic degradation of the glycocalix has no significant effect in PIU [13]. The glycocalix, though being a major contributor to the cell's ζ-potential, neither changes the surface electric charge on the cell's phospholipid bilayer nor shields it from the bulk medium pH [40]. These findings suggest that the ζ-potential is not a significant modulator of the PIU process.

4.2. The transmembrane proton concentration gradient does not affect PIU

The findings that the attenuation of the trans-membrane proton gradient has no direct effect on the extent of PIU, can be attributed to the asymmetrical lipid composition of the plasma membrane. The membrane outer leaflet is rich with zwitterionic phosphatydilcholine and sphingomyelin while the inner leaflet is rich with acidic phosphatydilserine and zwitterionic phosphatydilethanolamine. Though the zwitterionic polar head of lipids is basically electrically neutral, it is actually in equilibrium with cations and anions such as protons and hydroxide ions. When hydrogen ions are in excess, the protons bind to the negative phosphate group leading to the shift of the neutral polar head towards a cationic one. However, in more alkaline solutions, the hydroxide ion binds to the positive choline group shifting the polar head

group towards an anionic one. Thus, as solution pH varies, different concentrations of protons/hydroxide act as counterions to neutralize respectively either phosphate or choline groups on PC lipids, thereby altering their surface charge [41]. This difference in external and internal phospholipid composition dictates that the inner leaflet surface posses a more negative surface charge [42]. This results from the lower value of the isoelectric point (pI) of phosphatydilserine, (pI = 3.36) than those of sphingomyelin, phosphatydilcholine and phosphatydilethanolamine, possessing pI values of 4.01, 4.18 and 4.15, respectively [43,44]. As the membrane interface potential barrier largely depends on its surface proton buffering capacity [45], the aforementioned difference between two membrane leaflets' isoelectric points allows each leaflet to generate a different proton concentration at its surface, despite the equal pH of the bulk solutions [46]. Thus, exposure to identical bulk pH of 5.2 on both sides of the membrane has a higher impact on the charge of the PC as compared with that of the PS. We have previously proposed [13] that protons can act as counterions to the phospholipids acidic polarheads, consequently reducing the surface charge density and their mutual repulsion, resulting in excessive area asymmetry between the two lipid leaflets. This electro-mechanical instability can be compensated by the membrane adopting a negative spontaneous curvature, leading to the formation of a local folding. Due to the difference in their pK, the charge density of the membrane outer surface will be lower than its inner surface, allowing for the proton-induced membrane folding to take place.

4.3. The extent of PIU depends linearly on temperature

One of the characteristics of endocytosis is its attenuation at low temperature. Uptake through endocytic pathways was shown to be negligible below 10 °C. Above this temperature, endocytosis has biphasic character possessing a deflection point in the range of 20–24 °C [47–52]. Temperature affects the lipids in model bilayers by altering their conformation and packing order. At temperatures close to 0 °C, the lipid bilayer is at a lamellar gel phase where the alkyl chains are all in trans-configuration while the dipole lattice is disordered. When the membrane temperature is elevated the bilayer undergoes a phase transition that leads to the liquid-crystalline phase where considerable fraction of alkyl chain is disordered and the dipoles are aligned [53]. Unlike model lipid bilayers, the thermal-induced diversity within biological membranes is highly complex, as they contain diverse lipid species some of which may adopt a gel-phase while others a liquid-crystalline one. Attempts to characterize the phase behavior of biological membranes reveals broad intermediate phase transitions [54] commencing at 5 °C and extending up to 25 °C [55]. As a result, it is common to refer to the plasma membrane as consisting of two generalized lipid phases: high lipid ordered (L_O) or lipid disorder (L_D). The L_D phase is characterized by a low molecular order and high lipid mobility, which exhibits fast relaxation dynamics and a strong dipole. By contrast, the L_O phase is characterized by a higher molecular order, restricted lipid mobility and exhibits low dipole (i.e. low hydration).

For receptor mediated endocytosis, the activation energy below the deflection temperature (20–24 °C) is reported to be ~33–45 Kcal/mol and above it in the range of 12–18 Kcal/mol. These values were attributed to the sensitivity of membrane enzymes to the phase state of the lipid environment [48,51]. Many examples have been reported for temperature-dependent deflection in the activity of membrane associated enzymes. These include, for example, Na^+K^+-ATPase, Na^+/H^+-ion exchanger, Na^+ dependent transport systems for glucose, phosphate, prolin, taurin and *p*-aminohipurate, calcium transporters and chloride transporters [56]. For fluid phase endocytosis different data exist, where activation energy below the deflection temperature is relatively low (7–12 Kcal/mol) and higher above it (18–22 Kcal/mol). These findings were attributed to lipid raft clustering [57,58]. The kinetics of PIU as function of temperature differs from the reports above by being linear over the whole temperature range of 4–36 °C, devoid of any deflection point and possessing constant activation energy of 9.25 Kcal/mol (Fig. 4A). This difference supports the notion that PIU is not sensitive to enzymatic activity and raises the possibility that PIU is affected by parameters related more directly to the physico-chemical status of the lipid domains in the plasma membrane.

4.4. The cell membrane's fluidity and phase parameters affect the extent of PIU

PIU is proposed to depend on the membrane ability to adopt a new curvature in response to surface protonation [13]. The membrane curvature and elastic module are temperature dependent [59], as they involve the tilting movement of the hydrocarbon chains [60] and are thus correlated with membrane fluidity. The data shown in Fig. 4 indicates a linear correlation between the membrane fluidity and PIU. Variation in external pH between 7.4 and 5.2 produced no significant difference in the fluidity of the cell membrane, in the tested temperature range. This result is in line with previous reports showing that protonation can only induce lipid phase separation in the lipid bilayer in the low pH < 4 range [16,19,20,25].

When examining the data based on TMA-DPH anisotropy it should be taken into consideration that the trimethyl ammonium derivative of diphenyl hexatriene (TMA-DPH), ascertains anchorage of the fluorescent label to the membrane–water–lipid interface, aligns it perpendicular to the membrane plane, monitors the membrane anisotropy near the phospholipid head group region [61] and is not sensitive to cholesterol rich membrane domains [62]. Laurdan, on the other hand, distributes equally both in the gel and in the liquid-crystalline phases and does not associate itself with specific fatty acids or phospholipids head groups [25,63].

The results presented in this study could be explained through the perspective of membrane tension lines, as illustrated in Fig. 6. Membrane microdomains rich with cholesterol, sphingomyelin or glycosphingolipids have higher lipid order relative to that of the phospholipids bilayer [64,65]. These lipid microdomains possess different bending module and curvature than their surrounding phospholipid bilayer [66,67] and are thicker than the surrounding membrane [68,69]. This curvature and thickness mismatch can lead to an exposure of the hydrophobic membrane core to hydration, producing a pressure due to loss of acyl chain entropy within the hydrophobic domain. Compressive hydration forces acts at the hydrophilic interface to crowd the headgroups closer to minimizing exposure of the hydrophobic chains to water [8]. Using theoretical modeling of elastic and spatial parameters, it was demonstrated that, depending on the elastic deformation energy, phospholipid deformation can eliminate the hydrophobic contact with water [70]. The deformation energy per boundary length is defined by the line tension that separates the microdomain from its surrounding membrane. Line tension grows when microdomains and membrane spontaneous curvatures have the same sign (i.e. curving outward) [71] and the membrane at this intersection line adopts a negative spontaneous and elastic curvatures as function of the raft height to radius ratio [72]. Geometrically, it implies that at the line tension, the membrane curvature inverts and adopts a saddle shape, curving inward. We hypothesize that proton-induced membrane invaginations are initiated at these pre-existing tension lines separating thick L_O microdomains from the thinner surrounding L_D phospholipid membrane. Therefore, alteration of the phase order gradient or the membrane hydration pressure should affect the ability of proton-induced membrane asymmetry to initiate membrane budding. The concept has been demonstrated in giant unilamellar vesicles where pH gradient induce the formation of inside-protruding membrane tubes, detected at the L_D phase, only in the presence of GM1 L_O domains [20]. Once a membrane bud is formed, line energy can be reduced by shortening its contact boundary with the surrounding membrane [73]. The more the bud bulges out, its neck diameter shortens and its surface curvature becomes smaller; both parameters are energetically favorable since they reduce membrane tension [74]. The optimal shape that minimizes a

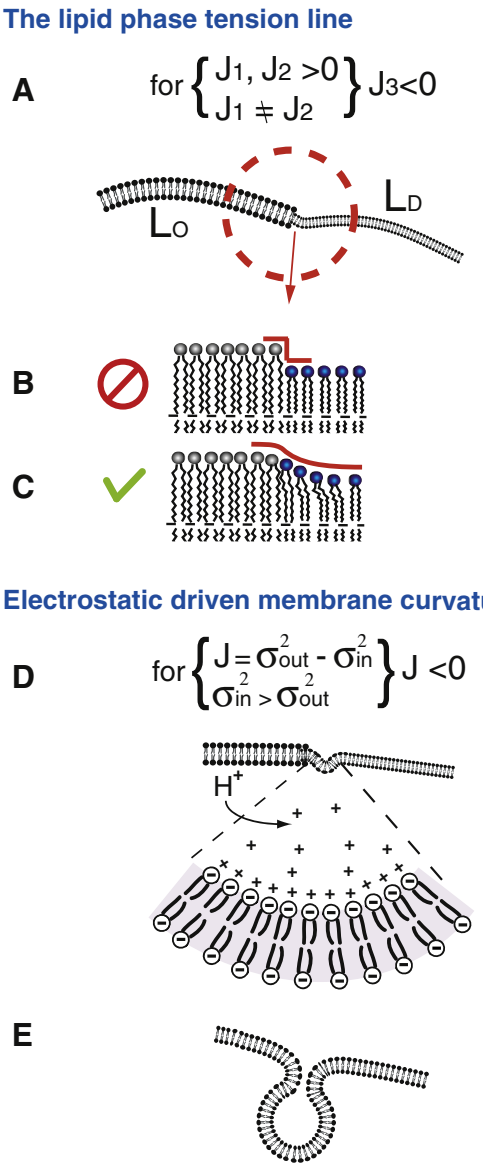

Fig. 6. Schematic model. (A) Lipid order phase (L_O) and lipid disorder phase (L_D) in the bilayer membrane vary by their bending module and spontaneous curvature, *J*. At the intersection of two different curvatures with the same sign (J_1, $J_2 > 0$), local curvature inverts ($J < 0$). (B) A width mismatch between the thicker L_O microdomain and the L_D phospholipid bilayer. (C) The phospholipids polar-heads deform to compensate the exposure of the hydrophobic tails to hydration, creating tension at the inversion line. (D) Smaller surface charge density (σ) reduce the electrostatic repulsion among the phospholipids acidic polar-heads in the external leaflet ($\sigma_{in} > \sigma_{out}$). The area asymmetry that develop between the bilayer leaflets increase the membrane tension which will deform locally where it is least stable, minimizing its energy state. (E) Tension energy is minimized by the membrane adopting a sphere shape and by constraining the tension line at the neck.

membrane tension is the sphere and the most mechanically stable form for a bud has the characteristic membrane neck [75,76]. Hence, there could be a thermodynamic preference for the formation of neck-connected membrane vesicles in response to external electrostatic charge manipulations, e.g. protonation of the phospholipid's acidic polar heads. A support for the involvement of lipid domains in endocytosis was recently described in the form of massive endocytosis (MEND) activated by both large calcium transients and amphipathic compounds [33,77]. Nonioinic detergents can induce MEND at concentrations > 100-fold, less than those used to isolate detergent resistant membranes. Calcium-activated and amphipath-activated MEND internalizes membrane domains that primarily contains ordered lipid in its outer monolayer. Apparently, the outer monolayer reorganizes to form lipid domains that spontaneously vesiculate inwardly, thereby fractionating the membrane in vivo [33]. These reports provide further evidence that lipid-related forces can drive physiological endocytic processes, although the identity of physiological MEND-promoting lipids remains to be established.

High order lipid microdomains are not passively equilibrated systems but are highly regulated by cytoskeleton remodeling and protein clustering [78,79]. Using electron paramagnetic resonance studies, it has been established that in the liquid-crystalline state cholesterol significantly increases the order of the phospholipid's hydrocarbon chains and restricts their rotation [80,81]. Indeed, we find that cholesterol enrichment of the cell's membrane elevates anisotropy and phase order (Fig. 5) of the L_D phase. The accompanied lower extent of PIU is explained by lowering the L_O/L_D gradient between the microdomains and the surrounding lipid bilayer. The depletion of membrane cholesterol, using MβC, had a small and insignificant effect on PIU, in agreement with an earlier report [13] and was shown to reduce the membrane packing order (Fig. 5B). However, it was also accompanied with lower membrane fluidity. This outcome could be explained by limited cholesterol depletion inflicting lipid microdomains segregation and dispersion rather than their degeneration, thereby increasing overall membrane rigidity [82,83].

Low concentrations of the detergent Tergitol were shown to increase membrane fluidity but reduce lipid packing order. The membrane properties of fluidity and packing order are not necessarily complementary [84], as the first depends on the rate of dipolar rotational motion and the second on the amplitude of rotational motion [32]. On one hand, Tergitol's long saturated alkyl tail can restrict the fluidic motion in the membrane but on the other hand, by partially dissolving L_O microdomains, it may reduce the L_O/L_D lipid phase gradient.

DMSO and phloretin have certain similar characteristics: both molecules are reported to affect the membrane packing density by increasing the area per lipid molecule, decreasing the bilayer thickness and partly dehydrating its surface [85–87]. Dehydration reduces the dipoles at the membrane surface which explains the elevated anisotropy in Fig. 5A. However, the two molecules differ in their influence on the membrane order (Fig. 5B). DMSO occupies the inner interface region, but due to its dual character it acts as a surfactant and stabilizes the presence of water molecules. Thus, DMSO partially dehydrates the lipid polar region but increases the water presence in the more inner parts of the membrane interface and increase cholesterol tilt orientation, reducing its ability to impose order in the membrane packing [88]. According to the tension line theory, the thinning of the phospholipids bilayer would be expected to enhance the mismatch at the boundary with the thicker, dense microdomains, and augment PIU, as indeed is the case with cells treated by phloretin (Fig. 5C). However, if DMSO can compromise the lipid's order, a reduced L_O/L_D lipid phase gradient at the microdomain's border would lower the tension line energy, with consequent lower extent of PIU.

Phospholipids are dipolar in character, due to the ester linkages between acidic head and the glycerol backbones. The alignment of these dipoles creates a charge separation which gives rise to an intramembrane dipole potential, $\Delta\psi_d$ [89]. 6KC, a cholesterol derivative in which additional keto group produces a large dipole moment, has been shown to intensify $\Delta\psi_d$ [90,91] as a result of uniform alignment of 6KC dipoles in the direction of the lipid ones. A higher $\Delta\psi_d$ is associated with increased reorientation of the dipoles [92] and a higher membrane fluidity (Fig. 5A). As polar surfaces in solvent are brought together, they experience a large repulsive interaction, termed the hydration pressure. In phospholipid membranes the magnitude of the hydration pressure is proportional to the square of the intramembrane dipole potential [93]. This increase in membrane surface hydration pressure is one of the forces that drive the phospholipids to distort and protect the hydrophobic core of the boundary thus having the ability to increase the tension line energy and consequently PIU.

It is important to note that phloretin effect on the membrane $\Delta\psi_d$ and the associated hydration pressure and lipid packing density is contrasting to that of 6KC, yet both these agents are able to promote an increase in PIU. This intriguing divergence may be owed to the fact that these contributions of 6KC and phloretin to the plasma membrane properties are not symmetrically opposed. At its fundamental state, the plasma membrane is at a dehydrated state, which allows 6KC to have a pronounced effect on membrane hydration pressure while phloretin can only have a limited dehydration range. As hydration pressure is proportional to the square of the dipole potential [93], this asymmetric proportionality is reflected by the 3:1 ratio between 6KC ability to increase the membrane dipole potential and phloretin ability to decrease it [90,91]. Along a similar reasoning, the fundamental high packing density of the membrane's phospholipids should be easier to expand rather than compress. Indeed phloretin can increase the area per lipid molecule of phosphatydilcholine bilayers (from approximately 64 $Å^2$ to about 78 $Å^2$ [94]), while 6KC does not markedly change the bilayer thickness or area per lipid molecule [95]. We reason that 6KC can increase PIU by elevating membrane hydration pressure, while phloretin increase PIU due to the expansion of the lipid packing as both these properties can contribute to the tension line energy at the L_O/L_D boundary. We may therefore deduce that PIU is governed by the membrane hydration and packing density rather than directly by $\Delta\psi_d$ itself.

In summary, the present study explores the involvement of membrane electric potentials in PIU and the contribution of membrane's lipid phases and fluidity to the uptake process is evaluated. We present evidence that the involvement of $\Delta\psi_m$ and ΔpH in PIU is mediated through reorganization of the actin cytoskeletal structure, in line with our earlier report [15]. The intramembrane dipole potential ($\Delta\psi_d$) has no direct effect over PIU, as both phloretin (which decreases $\Delta\psi_d$) and 6KC (which increases $\Delta\psi_d$) facilitated its increase. The first and critical step in producing vesicles from the plasma membrane is the formation of an inward curvature. In receptor-mediated endocytosis, this step is commonly governed by curvature-forming proteins. We suggest that in the case of PIU, membrane curvature is driven by the combination of lipid phase separation and an excessive cross-membrane surface area asymmetry. We demonstrate that the extent of PIU by cells in-vitro, can be manipulated by altering the plasma membrane lipid order and suggests that the critical parameter is the L_O/L_D gradient across the tension lines along the borders the condensed “rafts” microdomains.

References

[1] G.J. Praefcke, H.T. McMahon, The dynamin superfamily: universal membrane tubulation and fission molecules? Nat. Rev. Mol. Cell Biol. 5 (2004) 133–147.
[2] S. Mayor, R.E. Pagano, Pathways of clathrin-independent endocytosis, Nat. Rev. Mol. Cell Biol. 8 (2007) 603–612.
[3] G.J. Doherty, H.T. McMahon, Mechanisms of endocytosis, Annu. Rev. Biochem. 78 (2009) 857–902.
[4] S.A. Safran, Statistical Thermodynamics of Surfaces, Interfaces, and Membranes, Addison-Wesley, 1994.
[5] M.P. Sheetz, S.J. Singer, Biological membranes as bilayer couples. A molecular mechanism of drug–erythrocyte interactions, Proc. Natl. Acad. Sci. U. S. A. 71 (1974) 4457–4461.
[6] M. Winterhalter, W. Helfrich, Effect of surface charge on the curvature elasticity of membranes, J. Phys. Chem. 92 (1988) 6865.
[7] M. Winterhalter, W. Helfrich, Bending elasticity of electrical charged bilayers: coupled monolayers, neutral surfaces, and balancing stresses, J. Phys. Chem. 96 (1992) 327–330.
[8] P.A. Janmey, P.K. Kinnunen, Biophysical properties of lipids and dynamic membranes, Trends Cell Biol. 16 (2006) 538–546.
[9] Y. Li, B.Y. Ha, Molecular theory of asymmetrically charged bilayers: preferred curvatures, Europhys. Lett. 70 (2005) 411–417.
[10] H.W.G. Lim, M. Wortis, R. Mukhopadhyay, Stomatocyte–discocyte–echinocyte sequence of the human red blood cell: evidence for the bilayer-couple hypothesis from membrane mechanics, Proc. Natl. Acad. Sci. U. S. A. 99 (2002) 16766–16769.
[11] P. Galatola, Tube formation and spontaneous budding in a fluid charged membrane, Phys. Rev. E Stat. Nonlin. Soft Matter Phys. 72 (2005) 041930.
[12] V. Kumaran, Effect of surface charges on the curvature moduli of a membrane, Phys. Rev. E Stat. Nonlin. Soft Matter Phys. 64 (2001) 051922.
[13] N. Ben-Dov, R. Korenstein, Enhancement of cell membrane invaginations, vesiculation and uptake of macromolecules by protonation of the cell surface, PLoS One 7 (2012) e35204.
[14] N. Ben-Dov, I. Rozman Grinberg, R. Korenstein, Electroendocytosis is driven by the binding of electrochemically produced protons to the cell's surface, PLoS One 7 (2012) e50299.
[15] N. Ben-Dov, R. Korenstein, Actin-cytoskeleton rearrangement modulates proton-induced uptake, Exp. Cell Res. 319 (2013) 946–954.
[16] Y. Zhou, R.M. Raphael, Solution pH alters mechanical and electrical properties of phosphatidylcholine membranes: relation between interfacial electrostatics, intramembrane potential, and bending elasticity, Biophys. J. 92 (2007) 2451–2462.
[17] H. Hauser, Mechanism of spontaneous vesiculation, Proc. Natl. Acad. Sci. U. S. A. 86 (1989) 5351–5355.
[18] N. Khalifat, N. Puff, S. Bonneau, J.B. Fournier, M.I. Angelova, Membrane deformation under local pH gradient: mimicking mitochondrial cristae dynamics, Biophys. J. 95 (2008) 4924–4933.
[19] N. Khalifat, J.B. Fournier, M.I. Angelova, N. Puff, Lipid packing variations induced by pH in cardiolipin-containing bilayers: the driving force for the cristae-like shape instability, Biochim. Biophys. Acta 1808 (2011) 2724–2733.
[20] G. Staneva, N. Puff, M. Seigneuret, H. Conjeaud, M.I. Angelova, Segregative clustering of Lo and Ld membrane microdomains induced by local pH gradients in GM1-containing giant vesicles: a lipid model for cellular polarization, Langmuir 28 (47) (2012) 16327–16337.
[21] P. Boukamp, R.T. Petrussevska, D. Breitkreutz, J. Hornung, A. Markham, N.E. Fusenig, Normal keratinization in a spontaneously immortalized aneuploid human keratinocyte cell line, J. Cell Biol. 106 (1988) 761–771.
[22] T.J. Rink, R.Y. Tsien, T. Pozzan, Cytoplasmic pH and free Mg2 + in lymphocytes, J. Cell Biol. 95 (1982) 189–196.
[23] V.L. Mosiman, B.K. Patterson, L. Canterero, C.L. Goolsby, Reducing cellular autofluorescence in flow cytometry: an in situ method, Cytometry 30 (1997) 151–156.
[24] J.G. Kuhry, G. Duportail, C. Bronner, G. Laustriat, Plasma membrane fluidity measurements on whole living cells by fluorescence anisotropy of trimethylammonium-diphenylhexatriene, Biochim. Biophys. Acta 845 (1985) 60–67.
[25] T. Parasassi, G. De Stasio, G. Ravagnan, R.M. Rusch, E. Gratton, Quantitation of lipid phases in phospholipid vesicles by the generalized polarization of Laurdan fluorescence, Biophys. J. 60 (1991) 179–189.
[26] J.G. Fitz, T.E. Trouillot, B.F. Scharschmidt, Effect of pH on membrane potential and K + conductance in cultured rat hepatocytes, Am. J. Physiol. Gastrointest. Liver Physiol. 257 (1989) G961–G968.
[27] J.S. Stoddard, L. Reuss, pH effects on basolateral membrane ion conductances in gallbladder epithelium, Am. J. Physiol. Cell Physiol. 256 (1989) C1184–C1195.
[28] S.K. Keller, T.J. Jentsch, M. Koch, M. Wiederholt, Interactions of pH and K + conductance in cultured bovine retinal pigment epithelial cells, Am. J. Physiol. Cell Physiol. 250 (1986) C124–C137.
[29] K. Sandvig, T.I. Tonnessen, O. Sand, S. Olsnes, Requirement of a transmembrane pH gradient for the entry of diphtheria toxin into cells at low pH, J. Biol. Chem. 261 (1986) 11639–11644.
[30] S. Nobili, I. Landini, B. Giglioni, E. Mini, Pharmacological strategies for overcoming multidrug resistance, Curr. Drug Targets 7 (2006) 861–879.
[31] W.E. Lands, F.S. Davis, in: R.C. Aloia (Ed.), Membrane Fluidity in Biology, Academic Press, New York, 1983, pp. 1–4.
[32] L.W. Engel, F.G. Prendergast, Values for and significance of order parameters and “cone angles” of fluorophore rotation in lipid bilayers, Biochemistry 20 (1981) 7338–7345.
[33] M. Fine, M.C. Llaguno, V. Lariccia, M.J. Lin, A. Yaradanakul, D.W. Hilgemann, Massive endocytosis driven by lipidic forces originating in the outer plasmalemmal monolayer: a new approach to membrane recycling and lipid domains, J. Gen. Physiol. 137 (2011) 137–154.
[34] P.F. Almeida, A. Pokorny, A. Hinderliter, Thermodynamics of membrane domains, Biochim. Biophys. Acta 1720 (2005) 1–13.
[35] S. Chifflet, V. Correa, V. Nin, C. Justet, J.A. Hernandez, Effect of membrane potential depolarization on the organization of the actin cytoskeleton of eye epithelia. The role of adherens junctions, Exp. Eye Res. 79 (2004) 769–777.
[36] S. Chifflet, J.A. Hernandez, S. Grasso, A. Cirillo, Nonspecific depolarization of the plasma membrane potential induces cytoskeletal modifications of bovine corneal endothelial cells in culture, Exp. Cell Res. 282 (2003) 1–13.
[37] V. Nin, J.A. Hernandez, S. Chifflet, Hyperpolarization of the plasma membrane potential provokes reorganization of the actin cytoskeleton and increases the stability of adherens junctions in bovine corneal endothelial cells in culture, Cell Motil. Cytoskeleton 66 (2009) 1087–1099.
[38] S. Chifflet, J.A. Hernández, The plasma membrane potential and the organization of the actin cytoskeleton of epithelial cells, Int. J. Cell Biol. 2012 (2012), (ID 121424).
[39] D.C. Grahame, The electrical double layer and the theory of electrocapillarity, Chem. Rev. 41 (1947) 441–501.
[40] J.E. Schnitzer, Glycocalyx electrostatic potential profile analysis: ion, pH, steric, and charge effects, Yale J. Biol. Med. 61 (1988) 427–446.
[41] H.I. Petrache, T. Zemb, L. Belloni, V.A. Parsegian, Salt screening and specific ion adsorption determine neutral-lipid membrane interactions, Proc. Natl. Acad. Sci. U. S. A. 103 (2006) 7982–7987.
[42] R.M. Peitzsch, M. Eisenberg, K.A. Sharp, S. McLaughlin, Calculations of the electrostatic potential adjacent to model phospholipid bilayers, Biophys. J. 68 (1995) 729–738.
[43] A.D. Petelska, Z.A. Figaszewski, Effect of pH on the interfacial tension of bilayer lipid membrane formed from phosphatidylcholine or phosphatidylserine, Biochim. Biophys. Acta 1561 (2002) 135–146.
[44] A.D. Petelska, Z.A. Figaszewski, Effect of pH on the interfacial tension of lipid bilayer membrane, Biophys. J. 78 (2000) 812–817.

[45] D.A. Cherepanov, W. Junge, A.Y. Mulkidjanian, Proton transfer dynamics at the membrane/water interface: dependence on the fixed and mobile pH buffers, on the size and form of membrane particles, and on the interfacial potential barrier, Biophys. J. 86 (2004) 665–680.
[46] A.Y. Mulkidjanian, J. Heberle, D.A. Cherepanov, Protons @ interfaces: implications for biological energy conversion, Biochim. Biophys. Acta 1757 (2006) 913–930.
[47] R.C. de Figueiredo, M.J. Soares, Low temperature blocks fluid-phase pinocytosis and receptor-mediated endocytosis in *Trypanosoma cruzi* epimastigotes, Parasitol. Res. 86 (2000) 413–418.
[48] B.J. Iacopetta, E.H. Morgan, The kinetics of transferrin endocytosis and iron uptake from transferrin in rabbit reticulocytes, J. Biol. Chem. 258 (1983) 9108–9115.
[49] E.M. Muir, D.E. Bowyer, Dependence of fluid-phase pinocytosis in arterial smooth-muscle cells on temperature, cellular ATP concentration and the cytoskeletal system, Biochem. J. 216 (1983) 467–473.
[50] M.K. Pratten, J.B. Lloyd, Effects of temperature, metabolic inhibitors and some other factors on fluid-phase and adsorptive pinocytosis by rat peritoneal macrophages, Biochem. J. 180 (1979) 567–571.
[51] P.H. Weigel, J.A. Oka, Temperature dependence of endocytosis mediated by the asialoglycoprotein receptor in isolated rat hepatocytes. Evidence for two potentially rate-limiting steps, J. Biol. Chem. 256 (1981) 2615–2617.
[52] K. Sandvig, S. Olsnes, Effect of temperature on uptake, excretion and degradation of abrin and ricin by HeLa cells, Experimental cell research 121 (1) (1979) 15–25.
[53] S. Leekumjorn, A.K. Sum, Molecular studies of the gel to liquid-crystalline phase transition for fully hydrated DPPC and DPPE bilayers, Biochim. Biophys. Acta 1768 (2007) 354–365.
[54] P.W. Dijck, E.J. Zoelen, R. Seldenrijk, L.L. Deenen, J. Gier, Calorimetric behaviour of individual phospholipid classes from human and bovine erythrocyte membranes, Chem. Phys. Lipids 17 (1976) 336–343.
[55] D. Furtado, W.P. Williams, A.P. Brain, P.J. Quinn, Phase separations in membranes of *Anacystis nidulans* grown at different temperatures, Biochim. Biophys. Acta 555 (1979) 352–357.
[56] C. Le Grimellec, G. Friedlander, E.H. el Yandouzi, P. Zlatkine, M.C. Giocondi, Membrane fluidity and transport properties in epithelia, Kidney Int. 42 (1992) 825–836.
[57] Z. Mamdouh, M.C. Giocondi, R. Laprade, C. Le Grimellec, Temperature dependence of endocytosis in renal epithelial cells in culture, Biochim. Biophys. Acta 1282 (1996) 171–173.
[58] W.F. Wolkers, S.A. Looper, R.A. Fontanilla, N.M. Tsvetkova, F. Tablin, J.H. Crowe, Temperature dependence of fluid phase endocytosis coincides with membrane properties of pig platelets, Biochim. Biophys. Acta 1612 (2003) 154–163.
[59] D.P. Siegel, M.M. Kozlov, The gaussian curvature elastic modulus of N-monomethylated dioleoylphosphatidylethanolamine: relevance to membrane fusion and lipid phase behavior, Biophys. J. 87 (2004) 366–374.
[60] L.V. Chernomordik, M.M. Kozlov, Protein–lipid interplay in fusion and fission of biological membranes, Annu. Rev. Biochem. 72 (2003) 175–207.
[61] R.D. Kaiser, E. London, Location of diphenylhexatriene (DPH) and its derivatives within membranes: comparison of different fluorescence quenching analyses of membrane depth, Biochemistry 37 (1998) 8180–8190.
[62] Y.S. Jiang, Z.X. Jin, H. Umehara, T. Ota, Cholesterol-dependent induction of dendrite formation by ginsenoside Rh2 in cultured melanoma cells, Int. J. Mol. Med. 26 (2010) 787–793.
[63] L.A. Bagatolli, S.A. Sanchez, T. Hazlett, E. Gratton, Giant vesicles, Laurdan, and two-photon fluorescence microscopy: evidence of lipid lateral separation in bilayers, Methods Enzymol. 360 (2003) 481–500.
[64] G. Gupta, A. Surolia, Glycosphingolipids in microdomain formation and their spatial organization, FEBS Lett. 584 (2010) 1634–1641.
[65] D. Lingwood, K. Simons, Lipid rafts as a membrane-organizing principle, Science 327 (2010) 46–50.
[66] T. Baumgart, S.T. Hess, W.W. Webb, Imaging coexisting fluid domains in biomembrane models coupling curvature and line tension, Nature 425 (2003) 821–824.
[67] F. Julicher, R. Lipowsky, Domain-induced budding of vesicles, Phys. Rev. Lett. 70 (1993) 2964–2967.
[68] M. Gandhavadi, D. Allende, A. Vidal, S.A. Simon, T.J. McIntosh, Structure, composition, and peptide binding properties of detergent soluble bilayers and detergent resistant rafts, Biophys. J. 82 (2002) 1469–1482.
[69] C. Yuan, J. Furlong, P. Burgos, L.J. Johnston, The size of lipid rafts: an atomic force microscopy study of ganglioside GM1 domains in sphingomyelin/DOPC/cholesterol membranes, Biophys. J. 82 (2002) 2526–2535.
[70] S.A. Akimov, P.I. Kuzmin, J. Zimmerberg, F.S. Cohen, Y.A. Chizmadzhev, An elastic theory for line tension at a boundary separating two lipid monolayer regions of different thickness, J. Electroanal. Chem. 564 (2004) 13–18.
[71] P.I. Kuzmin, S.A. Akimov, Y.A. Chizmadzhev, J. Zimmerberg, F.S. Cohen, Line tension and interaction energies of membrane rafts calculated from lipid splay and tilt, Biophys. J. 88 (2005) 1120–1133.
[72] T.S. Ursell, W.S. Klug, R. Phillips, Morphology and interaction between lipid domains, Proc. Natl. Acad. Sci. U. S. A. 106 (2009) 13301–13306.
[73] M.F. Hanzal-Bayer, J.F. Hancock, Lipid rafts and membrane traffic, FEBS Lett. 581 (2007) 2098–2104.
[74] R. Lipowsky, Domains and rafts in membranes—hidden dimensions of self organization, J. Biol. Phys. 28 (2002) 195–210.
[75] T. Kosawada, K. Inoue, G.W. Schmid-Schonbein, Mechanics of curved plasma membrane vesicles: resting shapes, membrane curvature, and in-plane shear elasticity, J. Biomech. Eng. 127 (2005) 229–236.
[76] M. Lenz, S. Morlot, A. Roux, Mechanical requirements for membrane fission: common facts from various examples, FEBS Lett. 583 (2009) 3839–3846.
[77] D.W. Hilgemann, M. Fine, Mechanistic analysis of massive endocytosis in relation to functionally defined surface membrane domains, J. Gen. Physiol. 137 (2011) 155–172.
[78] A. Chaudhuri, B. Bhattacharya, K. Gowrishankar, S. Mayor, M. Rao, Spatiotemporal regulation of chemical reactions by active cytoskeletal remodeling, Proc. Natl. Acad. Sci. U. S. A. 108 (2011) 14825–14830.
[79] K. Gowrishankar, S. Ghosh, S. Saha, C. Rumamol, S. Mayor, M. Rao, Active remodeling of cortical actin regulates spatiotemporal organization of cell surface molecules, Cell 149 (2012) 1353–1367.
[80] D. Kurad, G. Jeschke, D. Marsh, Lateral ordering of lipid chains in cholesterol-containing membranes: high-field spin-label EPR, Biophys. J. 86 (2004) 264–271.
[81] D. Marsh, D. Kurad, V.A. Livshits, High-field spin-label EPR of lipid membranes, Magn. Reson. Chem. 43 (2005) S20–S25, (Spec no.).
[82] M. Hao, F.R. Maxfield, Characterization of rapid membrane internalization and recycling, J. Biol. Chem. 275 (2000) 15279–15286.
[83] S. Mahammad, J. Dinic, J. Adler, I. Parmryd, Limited cholesterol depletion causes aggregation of plasma membrane lipid rafts inducing T cell activation, Biochim. Biophys. Acta 1801 (2010) 625–634.
[84] G. M'Baye, Y. Mely, G. Duportail, A.S. Klymchenko, Liquid ordered and gel phases of lipid bilayers: fluorescent probes reveal close fluidity but different hydration, Biophys. J. 95 (2008) 1217–1225.
[85] R. Cseh, R. Benz, Interaction of phloretin with lipid monolayers: relationship between structural changes and dipole potential change, Biophys. J. 77 (1999) 1477–1488.
[86] A.A. Gurtovenko, J. Anwar, Modulating the structure and properties of cell membranes: the molecular mechanism of action of dimethyl sulfoxide, J. Phys. Chem. B 111 (2007) 10453–10460.
[87] V.I. Gordeliy, M.A. Kiselev, P. Lesieur, A.V. Pole, J. Teixeira, Lipid membrane structure and interactions in dimethyl sulfoxide/water mixtures, Biophys. J. 75 (1998) 2343–2351.
[88] M.A. de Menorval, L.M. Mir, M.L. Fernandez, R. Reigada, Effects of dimethyl sulfoxide in cholesterol-containing lipid membranes: a comparative study of experiments in silico and with cells, PLoS One 7 (2012) e41733.
[89] R.F. Flewelling, W.L. Hubbell, The membrane dipole potential in a total membrane potential model. Applications to hydrophobic ion interactions with membranes, Biophys. J. 49 (1986) 541–552.
[90] E. Gross, R.S. Bedlack Jr., L.M. Loew, Dual-wavelength ratiometric fluorescence measurement of the membrane dipole potential, Biophys. J. 67 (1994) 208–216.
[91] M.F. Vitha, R.J. Clarke, Comparison of excitation and emission ratiometric fluorescence methods for quantifying the membrane dipole potential, Biochim. Biophys. Acta 1768 (2007) 107–114.
[92] G. Le Goff, M.F. Vitha, R.J. Clarke, Orientational polarisability of lipid membrane surfaces, Biochim. Biophys. Acta 1768 (2007) 562–570.
[93] S.A. Simon, T.J. McIntosh, Magnitude of the solvation pressure depends on dipole potential, Proc. Natl. Acad. Sci. 86 (1989) 9263–9267.
[94] G.L. Jendrasiak, R.L. Smith, T.J. McIntosh, The effect of phloretin on the hydration of egg phosphatidylcholine multilayers, Biochim. Biophys. Acta Biomembr. 1329 (1997) 159–168.
[95] S.A. Simon, T.J. McIntosh, A.D. Magid, D. Needham, Modulation of the interbilayer hydration pressure by the addition of dipoles at the hydrocarbon/water interface, Biophys. J. 61 (1992) 786–799.